Initial stages of growth of Fe on $Cu_3Au(001)$ at low temperature: Formation of two-layer-thick islands

M. Canepa,* P. Cantini, C. Mannori, S. Terreni, and L. Mattera
Istituto Nazionale di Fisica della Materia (INFM) and CFSBT, Dipartimento di Fisica, Università di Genova, via Dodecaneso 33, I-16146 Genova, Italy
(Received 21 March 2000)

A He diffraction study on the initial stages of growth of Fe on $Cu_3Au(001)$ at 140 K is presented. The measurements provide evidence of a nonconventional growth mode. Indeed, the analysis of rocking curves, carried out through two independent methods, gives clear evidence of the formation of small islands that present a singular height $h=3.18\pm0.05$ Å, typical of a bilayer structure. As growth proceeds the mean distance between bilayer islands remains essentially constant (~ 25 Å) until coalescence. At coalescence of the first bilayer, growth evolves through nucleation of the third layer. Experimental data rule out interface disruption at deposition. A possible connection of the bilayer growth with recent studies on the influence of electron confinement on the growth morphology is proposed. Thermal treatments significantly affect the morphology of bilayer islands. In particular, annealing at room temperature induces an aggregation of islands. After annealing at 400 K a striking reassembling of the islands, which become three layers thick, is observed.

I. INTRODUCTION

It is well established that the structural and morphological stability of ultrathin heteroepitaxial films is strongly dependent on the strain induced by lattice mismatch.[1] Strained films may have magnetic properties that differ significantly from those of bulk phases[2] and are therefore most interesting from a fundamental point of view and also potentially appealing for technological innovation.

In this respect, the $Fe/Cu_3Au(001)$ system has recently attracted considerable attention as a case study in the field of the magnetic properties of tetragonally strained states of iron.[3–7] Previous studies on this system mostly focused on the properties of films grown at room temperature (RT). These studies report a scenario in which structural, morphological, and magnetic properties show a complex mutual relation.[7] Fe intermixing with substrate atoms, notably Au, seems to affect the growth morphology and magnetic properties of RT films[4]. A chemically sharp interface was obtained instead for deposition at lower temperatures (around 150 K). Nevertheless, even in the case of low temperature deposition, the experimental analysis was then mainly carried out after annealing at RT[4,7] and little information was given on as-deposited films. Taking into account that thermal treatments, even if mild, can significantly change the morphology (and the magnetic properties) of ultrathin films,[8] further investigation of the physical properties of metastable films just after deposition at low temperature seems highly desirable.

In this paper we present results on the growth at low temperature (LT, 140 K) of Fe on a well defined $Cu_3Au(001)$ substrate. We focused our attention on very initial stages of growth where information from previous work was scarce. Our He scattering experiment in the submonolayer range gives a clear evidence of a nonconventional growth mode that involves the formation of small, flat iron islands with a preferential height typical of a bilayer stack. This observation is, in our opinion, rather interesting for several reasons.

Bilayer-island growth seems hardly explainable in terms of strain-related concepts only. It rather recalls the influence of electron confinement effects in structural stabilization.[9,10] A possible interplay between strain and electron confinement effects has been suggested recently[9] and experimental findings such as those reported in this paper may trigger a discussion on such a stimulating point. Further, the observation of Fe ''particles'' of nanometric size on the surface might be closely related to the absence of hysteretic behavior reported in magneto-optic experiments previously performed on this system at submonolayer coverage.[4,6]

The paper is organized as follows. In Sec. II a brief account of experimental conditions and procedures is reported. Results are presented in Sec. III and discussed in Sec. IV. Concluding remarks are reported in Sec. V.

II. EXPERIMENT

Details of the multitechnique experimental apparatus and the substrate characterization can be found in Ref. 11 and Refs. 12–14, respectively.

In brief, the $Cu_3Au(001)$ surface was been prepared by sputtering and annealing cycles accurately monitored by He diffraction (HeD), low energy ion scattering (LEIS), and angle-resolved ultraviolet photoemission. The clean surface at 140 K exhibits a sharp $c(2\times2)$ diffraction pattern.[13,14] This pattern is representative of the Cu-Au termination of the so-called $L1_2$ bulk structure. Au and Cu atoms occupy the corners and the center of the surface conventional square cell (of side $a_{sub}=3.75$ Å), to give, on the average, a 50% Cu–50% Au composition.[15] From the morphological point of view, the surface is experienced by the helium atom probe as predominantly made of terraces a few hundred angstroms wide, separated by biatomic steps,[13] in agreement with previous determinations.[16]

Films were grown at $T_{dep}=140$ K. Fe was evaporated

 ©2000 The American Physical Society

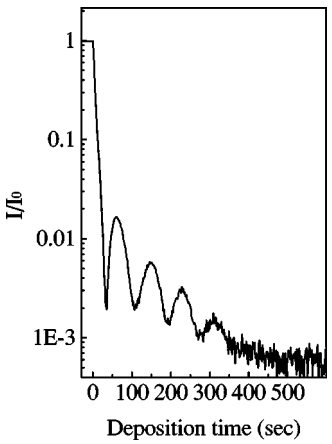

FIG. 1. Intensity of He reflectivity measured during deposition of Fe on $Cu_3Au(001)$ at 140 K. The zero of the time scale identifies the shutter opening. The reflectivity is normalized to its value prior to deposition (I_0).

from an electron bombardment source. HeD (wave vector $k_i = 5.87$ Å^{-1}, $\Delta k/k = 1\%$ full width at half maximum, kinetic energy $E = 17.9$ meV) was employed to monitor the film growth and to study the morphology of deposited films.[17]

Film deposition was controlled in real time by recording the intensity I of the specularly reflected He beam (in brief, HeR_{dep}). As in electron scattering experiments, HeR_{dep} patterns are useful for extracting information on growth regimes. Regular, well defined oscillations are usually considered as a fingerprint of layer-by-layer growth. Indeed, as far as He scattering is concerned, this situation is mostly encountered in homoepitaxial systems[18] or in surfactant-assisted growth.[19] In heteroepitaxial growth, HeR_{dep} patterns are generally more complex and their interpretation less straightforward.[20–22] Nevertheless, in less favorable cases also, HeR_{dep} patterns remain very useful as they allow a calibration of the deposition and a first qualitative insight into growth regimes.

In the present experiment, taking advantage of our previous experience on the Fe/Ag system, we measured HeR_{dep} at several angles of incidence (γ_i) of the He beam larger than 50° due to experimental constraints. In Fig. 1 the HeR_{dep} curve obtained at $\gamma_i = 67°$ is presented. The deposition curves, independently of γ_i, are mainly characterized by a strong damping indicative of a rapid accumulation of defects at the surface of the film. In Fig. 1, only a few weak yet well defined oscillations are superimposed on the damped regime. The detailed position and shape of the oscillations present a complex dependence on γ_i, as found in other heteroepitaxy experiments.[20,22] Qualitatively, the ensemble of deposition curves is representative of a rather complex mode of growth, in good agreement with a previous medium energy electron diffraction experiment.[4] Nevertheless, the extreme reproducibility of the curve of Fig. 1 verified over a great number of depositions gives us confidence that the same physical system is obtained upon stopping evaporation at the same point of the curve and allows a first estimate of the exposure. In this respect, we have assumed the average spacing between the maxima (or minima) of Fig. 1 to be representative of the deposition of one layer equivalent (1 LE). In this work we

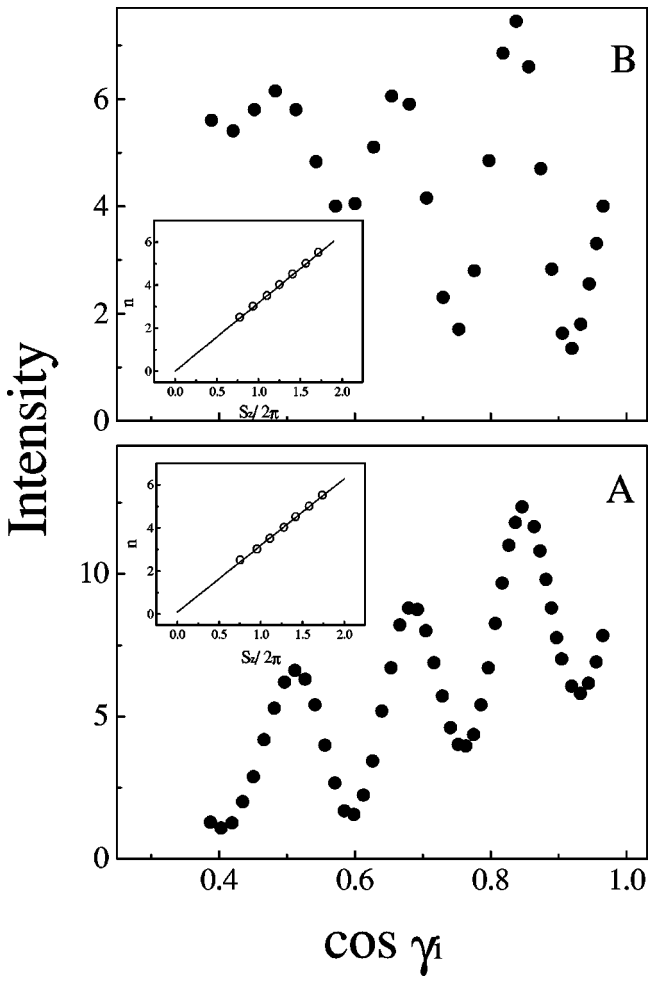

FIG. 2. He reflectivity measured as a function of the incidence angle of the beam (rocking curves). The curves were measured after having stopped deposition at (A) the first minimum and (B) the first maximum of the deposition curve of Fig. 1. In the insets the positions of maxima and minima of the rocking curves are reported in an n vs $S_z/2\pi$ plot (circles). The lines represent the best fit according to Eq. (2) (see text for further details of the values of fit parameters).

will concentrate our attention on films obtained after having stopped deposition at the first minimum (~ 0.5 LE) and at the first maximum (~ 1 LE) of the deposition curve of Fig. 1. The analysis of data carried out in the next sections will substantially confirm the first calibration of the exposure. Indeed, as growth initially proceeds through formation of bilayer islands, 0.5 LE will be found to correspond to a bilayer surface coverage of ~ 0.25.

III. RESULTS

In order to get more quantitative information on the growth mode we have studied the vertical terrace morphology of films, which is directly reflected in the ''rocking curve'' $I(S_z)$, i.e., the dependence of the helium specular intensity on the perpendicular momentum transfer $S_z = 2k_i \cos\gamma_i$. Figure 2 shows the $I(S_z)$ curves measured on (A) 0.5 and (B) 1 LE films. Both curves present well defined intensity oscillations related to interference paths of the He wave scattered from differently exposed levels. According to

kinematic theory, the angular positions of maxima (minima) should occur at $\cos\gamma_i$ satisfying the condition

$$S_z h = 2hk_i \cos\gamma_i = 2n\pi, \tag{1}$$

where h is the spacing between levels and n integer (half integer) corresponds to constructive (destructive) interference. In principle, deviations from the formula (1) can be expected in the case of heteroepitaxial systems, due to the presence of scatterers of different atomic nature. Yet deviations from Eq. (1) have been reported also in homoepitaxial systems, ascribed to the local strength of the He-surface interaction potential related to the presence of many small islands.[23,17] A simple attempt to account for such deviations can be made by introduction of a phase shift ϕ in Eq. (1):

$$S_z h = 2n\pi + \phi(k_i, \gamma_i). \tag{2}$$

If in a first-order approximation ϕ is assumed to be a constant, a linear fit of the positions of maxima and minima of the rocking curves in an n vs $S_z/2\pi$ plot can provide an estimate of the height h and an indication of the $\phi/2\pi$ correction, treated as free parameters. n vs $S_z/2\pi$ plots are presented in the insets of Fig. 2. A satisfactory fit was obtained giving $h_{0.5}^{LT}=3.12\pm0.05$ Å , $\phi_{0.5}^{LT}/2\pi=0.05\pm0.05$ and $h_1^{LT}=3.17\pm0.02$ Å, $\phi_1^{LT}/2\pi=0.02\pm0.02$.

Similar values of h^{LT} and $\phi^{LT}/2\pi$ are thus obtained for both films. The value of h^{LT}, if compared with the interlayer spacing of both unstrained and strained Fe structures (which ranges[1] between 1.435 and ~1.80 Å) and of Cu_3Au (1.875 Å), suggests that the islands are two layers thick. The values of $\phi^{LT}/2\pi$ turn out to be small, in contrast to what was found on other epitaxial systems;[23] this result instills some confidence in the use of kinematic approximations disregarding any phase correction.

In Fig. 2 the average specular intensity as a function of $\cos\gamma_i$, $I(S_z)$, increases [Fig. 2(a); 0.5 LE] or remains practically constant [Fig. 2(b); 1 LE]. This observation is in striking contrast with the decrease of $I(S_z)$ expected from the Debye-Waller effect and its exploration requires a quantitative analysis which will be reported in the next section.

The analysis of He reflectivity as a function of the parallel momentum transfer $I(\vec{S}_{||})$ can provide statistical information on the distribution of islands on the surface.[24] In Fig. 3 diffraction patterns taken along the $\langle 001\rangle$ substrate azimuth under the antiphase interference condition ($\cos\gamma_i=0.77$) are reported for (A) 0.5 and (B) 1 LE films. In panel A, a well defined small peak at $\vec{S}_{||}=-1.68$ Å^{-1} is detected at the position of the superlattice diffraction peak of the $c(2\times2)$ structure typical of the $Cu_3Au(001)$ substrate; its intensity decreases with increasing coverage but the peak is still visible at 1 LE. Considering the exclusive sensitivity of HeD to the topmost layer, this peak seems to derive from portions of the substrate that are not covered by iron. The broad shoulders at the sides of the specular peak provide information on the length scale Λ of the island-island separation or of the island size distributions.[25,26] The $\vec{S}_{||}$ position of the ''satellites'' (~0.25 Å^{-1}) turns out to be practically independent of coverage in the 0.5–1 LE range; further, diffraction patterns sampled along other azimuthal directions suggest an isotropic island distribution. These findings force us to assign the resulting Λ (~25 Å) to the average distance between islands. This assignment is consistent with a model where, after an initial nucleation stage and until coalescence, the number density of islands remains approximately constant while the island size increases.[27] Considering the island-island separation extracted from diffraction patterns, a first, effective estimate of the mean island size as a function of coverage can be deduced using a simple picture in which two-layer-thick square islands nucleate and expand around the corners of a square grid. From $\Lambda\sim25$ Å, the island size turns out to range from ~8 Å at 0.5 LE to ~12 Å at 1 LE.

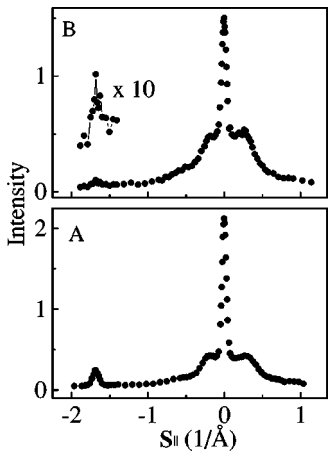

FIG. 3. Diffraction patterns obtained after stopping deposition at (A) the first minimum and (B) the first maximum of the deposition curve of Fig. 1. The profiles were measured in antiphase conditions, at 140 K.

In order to check the stability of the deposit against temperature variations, we investigated the morphology of the 1 LE film after mild annealing. Rocking curves taken upon annealing at RT and 400 K are presented in the upper and lower panel of Fig. 4, respectively. Representative spot profiles, measured under antiphase conditions, are shown in the top panel (RT) and in the lower panel (400 K) of Fig. 5, to be compared with the patterns of Fig. 3(b).

The fit of the positions of maxima and minima of the rocking curve of Fig. 4 (upper panel) through Eq. (2) provides an island height $h_1^{RT}=3.40\pm0.05$ Å with a phase $\phi_1^{RT}/2\pi=0.27\pm0.05$. A comparison of the upper panel of Fig. 5 with Fig. 3(B) shows that satellites come closer to the specular peak ($\vec{S}_{||}\sim0.15$ Å^{-1}) indicating an increase of the mean separation of islands ($\Lambda\sim40$ Å) and resulting in an estimated island size of ~20 Å.

Annealing at 400 K produces striking changes, as is immediately obvious on looking at the increased number of intensity oscillations of the rocking curve in the lower panel of Fig. 4. The period of the oscillations observed in the pattern, through Eq. (2), indicates a larger value of the island height $h_1^{400\ \mathrm{K}}=5.37\pm0.04$ Å accompanied by a quite large value of $\phi_1^{400\ \mathrm{K}}/2\pi=0.43\pm0.05$. In the spot profile of Fig. 5(B) the satellites of the specular peak are no longer resolved. Taking into account the diffractometer resolution, an island separation of at least 60–70 Å can be estimated.

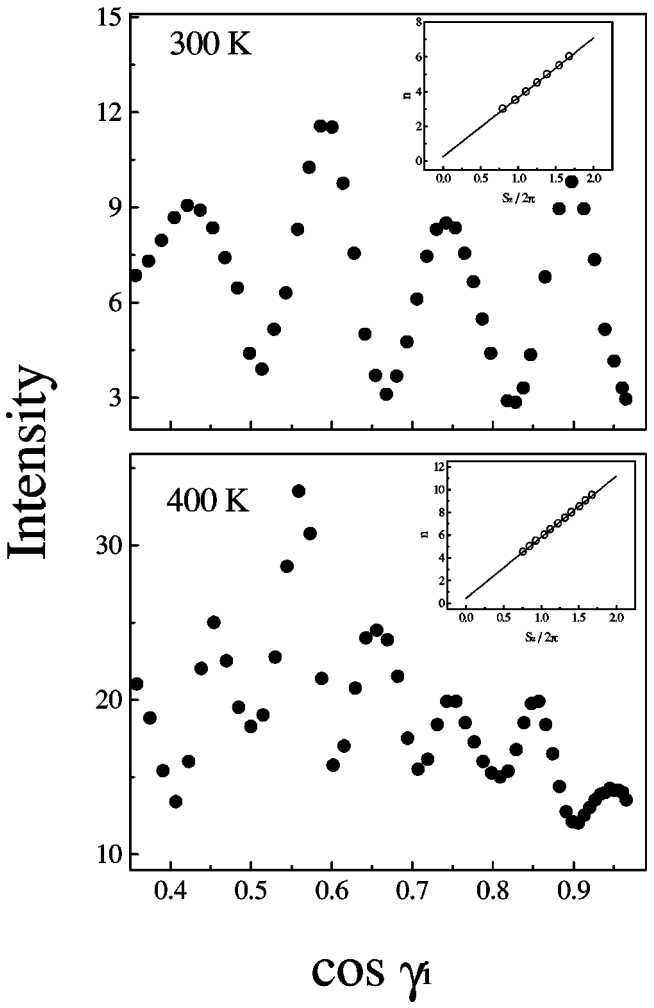

FIG. 4. Rocking curves measured after having stopped LT deposition at the first maximum of the deposition curve of Fig. 1 and after subsequent annealing to 300 K (top panel) and 400 K (lower panel). In the insets the positions of maxima and minima of the rocking curves are reported in an n vs $S_z/2\pi$ plot (circles). The lines represent the best fit according to Eq. (2).

IV. DISCUSSION

A. Surface vertical morphology

For a two-level system of terraces separated by steps of height h, θ_0 and θ_1 being the coverages of level 0 (substrate) and level 1 (islands), respectively, the specular intensity can be expressed as

$$I(\vec{S})=\{\exp[-\alpha(T)S_z^2]A(\vec{S}_{||})[\theta_0^2+\theta_1^2+2\theta_0\theta_1\cos(S_z h)]\}$$
$$+\{\exp[-\alpha(T)S_z^2]B(\vec{S}_{||})2\theta_0\theta_1[1-\cos(S_z h)]\}. \quad (3)$$

In Eq. (3) the first and second term in braces represent the δ-like and broad components of the Bragg peak, respectively. $A(\vec{S}_{||})$ is the instrumental response of the diffractometer and $B(\vec{S}_{||})$ is the Fourier transform of the step-step correlation function convoluted with $A(\vec{S}_{||})$). Formally, the exponential term represents the Debye-Waller attenuation of the intensity due to thermal vibrations. Equation (3) alone is not sufficient to reproduce the experimental data presented in Fig. 2. The average trend of the intensity at 0.5 and 1 LE exhibits a behavior that is opposite to what is expected from the Debye-Waller effect and cannot be accounted for by Eq. (3), independently of the number of levels considered in the model. The origin of such unusual patterns can be understood through the introduction of a *shadowing effect*: In a semiclassical view, tall islands prevent the He incoming wave at grazing incidence from reaching the substrate; in the same way, an outgoing wave with grazing **k** vector will not reach the detector.

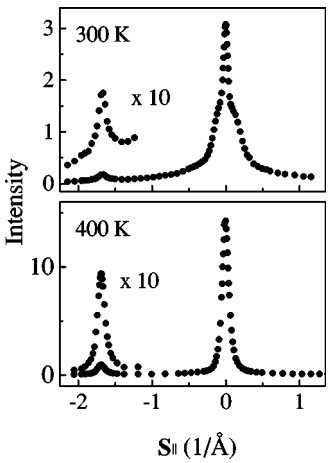

FIG. 5. Diffraction patterns measured after having stopped LT deposition at the first maximum of the deposition curve of Fig. 1 and after subsequent annealing to 300 K (top panel) and 400 K (lower panel).

For a two-level system the shadowing effect can be introduced by assuming that only a fraction of the lower level, say θ_0^*, contributes to the scattering amplitude, so that Eq. (3) is modified as follows:

$$I=A\exp[-\alpha S_z^2]$$
$$\times\left[\theta_0^{*2}+\theta_1^2+2\theta_0^*\theta_1\frac{B}{A}+2\theta_0^*\theta_1\left(1-\frac{B}{A}\right)\cos(S_z h)\right]. \quad (4)$$

Each island of height h shadows the substrate either for the incoming or the outgoing wave so that the shadowed area $\mathcal{A}_{sh}$ can be expressed by

$$\mathcal{A}_{sh}=2sh\tan\gamma',$$

where s is the size of the island perpendicular to the x-z scattering plane and $\tan\gamma'=k_x/k_z$. Taking into account the so-called Beeby correction,[28] the incident and outgoing wave vectors near the surface can be expressed as $\mathbf{k}_i\equiv(k\sin\gamma,0,-k\varepsilon)$ and $\mathbf{k}_f\equiv(k\sin\gamma,0,k\varepsilon)$, respectively, where ε $\varepsilon=\sqrt{\cos^2\gamma+\mathcal{D}/E}$; then it follows that $\tan\gamma'=k\sin\gamma/k\varepsilon$. In the previous expressions $\mathcal{D}$ is the effective well depth of the He-surface interaction potential.

The shadowed coverage can then be expressed as

$$\theta_{sh}=n\mathcal{A}_{sh}=2n\bar{s}h\tan\gamma',$$

where n is the island density and $\bar{s}$ the mean island size. Finally, the effective coverage of level 0 is

$$\theta_0^*=\theta_0-\theta_{sh}=\theta_0-2n\bar{s}h\tan\gamma'.$$

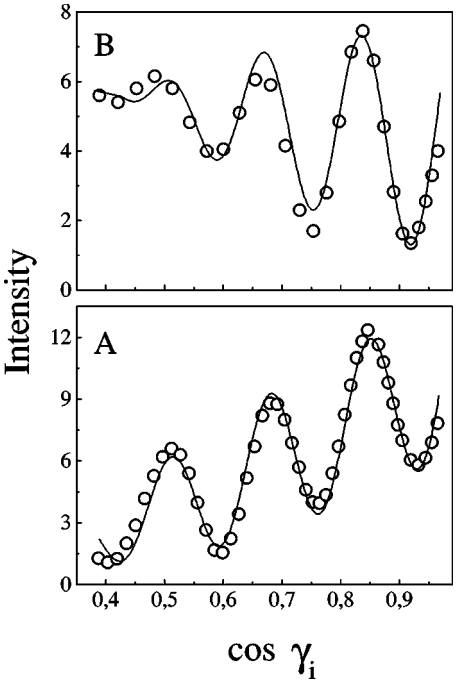

FIG. 6. Comparison between experimental rocking curves of Fig. 2 and the best fit of Eq. (4) to the data (see text for major details).

Equation (4), which describes the two-level system including the shadowing effect, was then used to fit the experimental data at 0.5 LE and 1 LE. A, α, θ_0, $\kappa = n\bar{s}$, B/A, and h were treated as adjustable parameters.

The comparison between the data at 0.5 LE and the calculated intensity is reported in Fig. 6(A). The fit provides a satisfactory agreement with the experimental data. The best fit values of the adjustable parameters are $A = 46.7$ a.u., $\alpha = 0.007$ Å^2, $\theta_0 = 0.80$, $n\bar{s} = 0.09$ Å^{-1}, $B/A = 0.22$, and $h_{0.5}^{LT} = 3.14$ Å. The coverage $\theta_1 = 1 - \theta_0 \sim 0.2$ is consistent with the value expected at ~ 0.5 LE in the case of bilayer growth. We note that, assuming again a picture of square islands ~ 25 Å apart, from $n\bar{s} = 0.09$ Å^{-1} a value of $\bar{s} = \theta_1 / n\bar{s} \sim 3$ Å is obtained, smaller than that derived from the spot profile analysis of the previous section.

The best fit curve obtained at 1 LE for $A = 20.3$ a.u., $\alpha = 0.006$ Å^2, $\theta_0 = 0.43$, $n\bar{s} = 0.06$ Å^{-1}, $B/A = 0.1$, and $h_1^{LT} = 3.19$ Å is shown as a continuous line in Fig. 6(B). The portion of the substrate covered by the islands, $\theta_1 = 1 - \theta_0 \sim 0.57$, is consistent with the value expected at ~ 1 LE in the case of bilayer growth. The value of the ratio B/A turned out lower than for the 0.5 LE film: The surface as a whole appears less rough. From $n\bar{s} = 0.06$ Å^{-1} a value of $\bar{s} = \theta_1 / n\bar{s} \sim 10$ Å is obtained, only slightly smaller than the value obtained from spot profiles.

Some further comments on the model are necessary.

In the fit, the value of $\mathcal{D}$ has been kept fixed to an effective value $\mathcal{D} = 8$ meV.[29] Different values of $\mathcal{D}$ lead to the same fit value of h within 0.01 Å. However, it must be noted that $\mathcal{D}$, as expected, is correlated to the values of α and of $n\bar{s}$. In particular, a lower value of $\mathcal{D}$ leads to lower values of both α and $n\bar{s}$. We note that the fit overestimates the product $n\bar{s}$ (and therefore the shadowed coverage θ_{sh}). This seems particularly true at 0.5 LE, where islands are smaller. Equations (4) and (3) do not account for the scattering intensity that is diffused out of the specular direction due to island edges, random vacancies, or adatoms. However, the parameter θ_{sh}, which removes intensity from the specular direction too, is partially charged with these diffusion effects. Therefore scattering of He by island edges leads to the overestimation of θ_{sh} and it is not surprising that this effect is more pronounced at 0.5 LE.

Nevertheless, the introduction of the shadowing effect effectively reproduces the average behavior of the specular intensity and allows us to emphasize the oscillating contribution related to steps at LT. We therefore remark on two important findings of our analysis. First, the value of h obtained in the fits turns out not to be correlated with the other parameters. The fits at 0.5 and 1 LE provide two very close values for h; it is worth noting that these values are absolutely consistent with those obtained in the much simpler analysis reported in the previous section. Second, a Fourier component alone reproduces the data accurately, corresponding to a peaked distribution of the height of islands. Interference oscillations related to bilayer islands are detected in rocking curves up to 1.2 LE; already at ~ 1.6 LE the rocking curve shows an interference pattern (not shown) related to monatomic steps instead [$h_{1.6}^{LT} = 1.9 \pm 0.1$ Å ; $\phi_1^{LT} = 0.05 \pm 0.10$ (Ref. 12)]. As their size increases, bilayer islands likely provide a substrate for nucleation of the third level.

As mentioned above, no phase shifts are observed in the rocking curves of Fig. 2 for the LT 0.5 and 1 LE films. A phase shift occurs instead after annealing and, unlike previous experiments on other systems[30,23] it gets stronger as the average size of islands increases. An important factor driving the shift $\phi(k_i, \gamma_i)$ is the local variation of the well depth $\mathcal{D}$, which is related to both the different nature of scatterers[20] (Fe on top of the islands, Cu and Au at the substrate level) and the small dimensions of the islands.[23] According to the present experimental results, these two factors seem to compete in the system under investigation leading to an effective cancellation of the phase shifts at LT.

The analysis of rocking curves illustrated in this section substantially confirms the calibration of the exposure given in Sec. II. Nucleated islands of bilayer height cover about 20% and 50% of the surface at 0.5 LE and 1 LE, respectively. Further, the rocking curves allow us to reconsider the behavior of the HeR_{dep} curve of Fig. 1 at the initial stages of deposition. Let us consider in Fig. 2 the intensity of minima (antiphase). At low γ_i the intensity at 1 LE turns out to be lower than that at 0.5 LE, as expected in the case of bilayer growth; at large γ_i, instead, where the shadowing becomes more and more effective, the intensity at 1 LE becomes greater. Therefore, the first maximum of the deposition curve, which has been measured at $\gamma_i = 67°$, arises from the closure of destructive interference paths due to shadowing. Subsequent maxima in the deposition curve, where monatomic steps are observed in rocking curves, rather reflect the completion of a (faulty) layer.

Obviously, a comparison with scanning tunneling microscopy (STM) measurements under similar experimental conditions would be most helpful to confirm our speculations and to provide more detailed information on the actual contours of islands. In this respect it is interesting to consider

recent STM measurements on this system[7] with the caution in mind that a close comparison with our results is not straightforward, because the measurements of Ref. 7 were focused on slightly thicker films and were taken after annealing at room temperature. Nevertheless, the STM pictures of the thinnest film investigated (2.2 LE deposited at 160 K and annealed at RT) show the presence of small size islands (a few tens of angstroms), of rather regular shape. A layer filling of 46%, 88%, and 96% is claimed for the third (topmost level), second, and first layer, respectively. Only 4% of the substrate remains uncovered. The STM measurements are therefore compatible with our bilayer model. In fact, according to our picture, at 2.2 LE the bilayer islands should essentially cover the substrate (note that the first and second layers have a very similar filling in STM data) and nucleation of the third layer is already started. Furthermore, a value of 1.9 ± 0.2 Å is reported in Ref. 7 for the height of the third level, consistent with our value of $h_{1.6}^{LT}$.[12]

B. Island structure and composition

Helium diffraction does not give immediate information on the composition and the ''internal'' geometric structure of the bilayer islands. In this respect, it is worth noting that LEIS measurements indicate that the signal of ions backscattered from Au and Cu atoms essentially vanishes at ~ 2 LE,[12] in good agreement with the layer occupancies detected in the STM measurements just mentioned,[7] and suggest the absence of intermixing at LT, in agreement with Auger measurements of Ref. 4.

The island height h found by HeD, if compared with the edge of the conventional cubic cell of both bcc (2.86 Å) and fcc (~ 3.6 Å) iron, indicates a strained structure. The strain is not surprising as the in-plane lattice constant of the substrate (2.65 Å) differs significantly from those of bcc and fcc iron (2.86 Å and ~ 2.56 Å). It seems therefore interesting to set up experiments to measure the geometric structure inside the islands with more local probes. In this respect an ion backscattering experiment is in progress and an x-ray photoelectron scattering experiment is planned.

C. Island stability versus temperature

The data obtained for the annealed 1 LE film indicate significant changes of the dimensions of the islands. The changes are already appreciable at RT. The position of the shoulders of the specular peak (Fig. 5; top panel) indicates in fact an increase of the mean separation of islands up to $\Lambda \sim 40$ Å, presumably related to some island aggregation. The simple analysis of rocking curves reported in Sec. III indicates a slight vertical expansion of the structures from $h_1^{LT} = 3.19 \pm 0.05$ Å to $h_1^{RT} = 3.40 \pm 0.05$ Å. The presence of a sizable phase shift in the rocking curve, however, should induce some caution about this result. The value of h was in fact obtained assuming the phase shift in Eq. (2) to be constant, independent of S_z; this approximation is not fully satisfactory and can introduce a systematic uncertainty, which, taking advantage of our experience on the Fe/Ag system,[23] can be estimated to be of the order of 0.1 Å . A more reliable treatment, accounting for a two-level system and an S_z-dependent phase shift as was done in Ref. 23, was able to reproduce accurately the positions of maxima and minima of the rocking curve with $h \simeq 3.45$ Å; however the model was still not satisfactory concerning the reproduction of the intensity, suggesting that a single value of the step height h is no longer sufficient for the annealed film.

As mentioned above, the changes in the rocking curve for the annealing at 400 K are striking. The value of h obtained from a simple analysis of the rocking curve unambiguously indicates the passage from a bilayer to a trilayer morphology. The increase of the intensity of both the $(\bar{1},0)$ and $(0,0)$ diffraction peaks (by a factor of 5 if compared to those measured at RT) is consistent with a larger substrate area left uncovered, which retains the $c(2\times 2)$ structure of the bare substrate. This observation seems to rule out interface disruption at deposition and after annealing at 400 K. Therefore, although LEIS data obtained at 400 K do not allow us to rule out a limited degree of segregation of substrate atoms on top of the islands, island reassembling seems to be preferentially related to the position of some iron on top of bilayer islands. The island reassembling and structural changes might be induced by the relief of the strain energy accumulated upon island aggregation.

D. Connection to electronic growth

Regarding metal-on-metal heteroepitaxy, the formation of islands of bilayer height has been reported in very few cases. A remarkable example is provided by the growth of Co on Au(111) (Ref. 31) and Cu(111).[32] For both systems, single-layer islands are only exceptionally observed in real-space STM images. For Co on Au(111) the formation of bilayer islands, which is claimed to reduce the total strain energy, is ascribed to the large (13%) mismatch between deposit and substrate.[31] In the case of Co on Cu(111), twinned bilayer islands of triangular shape are observed on all terraces imaged. In this case the mismatch is not large but the presence of twin-related orientation seems to play a role in the growth by yielding grain boundaries between Co crystallites.[32]

Simultaneous growth of the first two layers is claimed also in the initial stages of growth of Ni on W at RT.[33] It is interesting to note that these two materials are excellent candidates for forming metallic superlattices with an atomically abrupt interface. Furthermore, growth of bilayers observed at 150 K for the Pb/Cu(111) system only along with well defined film thicknesses[34] was attributed to a quantum size effect.

A recent study focusing on metal/semiconductor systems indicates height selection associated with electron confinement as a factor in structural and morphological stabilization of ultrathin films.[9] Such an ''electronic growth'' model has been invoked to explain the formation of bilayer plateaulike islands, recently demonstrated for the growth of Ag on Si(111).[10] It is interesting to note that electronic confinement is suggested to play a role also in metal-on-metal heteropitaxy [such as Pb on Cu(111)], provided that a sharp interface is formed.[9]

In this respect, our experiment provides a clear example of bilayer metal islands grown on a noble metal substrate; the presence of monolayer height islands seems statistically irrelevant as there is no trace of them in rocking curves up to 1.6 LE. In addition, we note that in our case the atomic

interface seems rather abrupt at low temperature. Finally, it is interesting to observe that Fe and Cu_3Au possess a dissimilar band structure, a condition that is necessary to drive electron confinement.[36] In fact, the *d* bands of iron, concentrated close to the Fermi energy, are decoupled from the *d* bands of Cu_3Au, located below 2 eV of binding energy.[35] Therefore, on the basis of all these considerations it is tempting to invoke *d*-electron confinement as a factor that contributes to lowering the surface energy in the formation of two-layer-high islands (in this case as probably also for Co on Cu and Au).

E. Connection to magnetic properties

There is still debate in the literature about the actual structure and magnetization of ultrathin Fe films on $Cu_3Au(001)$ as a function of thickness.[4,5,7] Concerning specifically the magnetic measurements, it is interesting to observe that the two experiments available on the magnetization of films deposited at LT are in substantial agreement about the onset ($\sim$1 LE) of the hysteretic behavior in Kerr measurements.[7,4] Above this coverage the film shows a magnetization perpendicular to the surface; the saturation values of the magnetization increase linearly up to a critical thickness λ_s where a spin reorientation transition takes place (the magnetization switches in a plane parallel to the surface). The values of λ_s show a clear dependence on the temperature of deposition and are somewhat scattered in the different experiments. Under experimental conditions apparently similar to those of our experiment, a value of $\lambda_s \sim 3$ LE has been reported.[4]

Our results raise an interesting question about the relation between the morphology and the magnetic properties of the deposit. The paramagnetic behavior reported in the earlier stages of growth could in fact be related to the limited size of islands and/or to their distribution on the surface.[37] In turn, the onset of the magnetization could be related to the achievement of a threshold in the size of islands, which become sufficiently large to sustain ferromagnetic behavior.

In this respect, and in connection with the notes on electronic growth reported above, it seems interesting to note that in the case of Co growth on Au(111) also the formation of perpendicular magnetic domains at coverage $\geqslant 2$ monolayers is qualitatively correlated with the observation of the coalescence of Co islands over large regions at this coverage.[31] In the case of growth of Co on Cu(111) in contrast, bilayer islands do not coalesce at higher coverages and growth evolution results in a granular film; this fact is claimed to explain the difficulty in the detection of antiferromagnetic coupling in Co/Cu(111) superlattices.[32]

V. CONCLUSIONS

He scattering measurements offer insight into the early stages of growth of Fe on $Cu_3Au(001)$ at 140 K. Diffraction measurements provide evidence of the nucleation of small islands (a few tens of angstroms). The experiment was focused on the study of the vertical morphology of these islands, reflected in the ''rocking curve'' $I(S_z)$, e.g., the dependence of the helium specular intensity on the perpendicular momentum transfer $S_z = 2k_i \cos \gamma_i$. Rocking curves measured on submonolayer films present in fact strong intensity oscillations related to interference paths of the He wave scattered from different exposed levels. The analysis of these rocking curves, carried out through two independent methods, gives clear evidence that nucleated islands present a singular height. Both models employed indicate an island height of the order of 3.2 Å, which is typical of a two-layer-thick structure (bilayer growth). Bilayer growth proceeds up to an exposure of 1.2 LE; already at $\sim$1.6 LE the rocking curve shows an interference pattern related to monatomic steps, indicating nucleation of the third layer.

Bilayer islands are not stable as the temperature is raised. At 1 LE, annealing at RT seems to induce some island aggregation accompanied by a slight expansion of the island height, whereas annealing at 400 K induces an evident aggregation and reassembling of the islands which become three layers thick.

We discussed the connection of our results on growth morphology with the electronic and magnetic properties of films. In this respect, our experiment, providing a clear example of growth of islands with a strongly preferred height, could stimulate investigations of the interplay between strain and genuine electronic processes in the stabilization of transition metal films on noble metal substrates. The possible relation of the limited size of islands with the absence of any hysteretic behavior at coverage lower than 1.1 ML, reported in several previous experiments, is a point that deserves further experimental investigation by a combined analysis with spin polarized metastable deexcitation spectroscopy[38] and Kerr effect measurements.

ACKNOWLEDGMENTS

The authors are most grateful to Professor Giovanni Boato for stimulating discussions and to A. Gussoni for helpful technical support. Financial support from MURST (Grant No. 9702178261_003) is acknowledged.

*Corresponding author: Email canepa@fisica.unige.it

[1] F. Jona and P.M. Marcus, Surf. Rev. Lett. **3**, 1285 (1996); P.M. Marcus and F. Jona, *ibid.* **1**, 15 (1994).

[2] M. Wuttig, B. Feldmann, and T. Flores, Surf. Sci. **331-333**, 659 (1995); T. Takahashi and W.A. Basset, Science **145**, 483 (1964); V.L. Moruzzi, P.M. Marcus, and J. Kübler, Phys. Rev. B **39**, 6957 (1989).

[3] R. Rochow, C. Carbone, Th. Dodt, F.P. Johnen, and E. Kisker, Phys. Rev. B **41**, 3426 (1990).

[4] B. Feldmann, B. Schirmer, A. Sokoll, and M. Wuttig, Phys. Rev. B **57**, 1014 (1998).

[5] B. Schirmer, B. Feldmann, and M. Wuttig, Phys. Rev. B **58**, 4984 (1998).

[6] M.-T. Lin *et al.*, Phys. Rev. B **55**, 5886 (1997).

[7] M.-T. Lin *et al.*, Surf. Sci. **410**, 290 (1998).

[8] D. Tillmann and E. Kisker, Solid State Commun. **100**, 415 (1996).

[9] Z. Zhang, Q. Niu, and C. Shih, Phys. Rev. Lett. **80**, 5381 (1998).

[10] L. Gavioli, K.R. Kimberlin, M.C. Tringides, J.F. Wendelken, and Z. Zhang, Phys. Rev. Lett. **82**, 129 (1999).

[11] M. Canepa *et al.*, Rev. Sci. Instrum. **62**, 1431 (1991).

[12] C. Mannori, Ph.D. thesis, University of Genova, 1998 (in English).
[13] C. Mannori, T. Scimia, P. Cantini, S. Terreni, M. Canepa, and L. Mattera, Surf. Sci. **433**, 307 (1999).
[14] C. Mannori, G. Boato, M. Canepa, P. Cantini, L. Mattera, and S. Terreni, Europhys. Lett. **45**, 686 (1999).
[15] W.E. Wallace and G.J. Auckland, Surf. Sci. Lett. **275**, L685 (1992).
[16] H. Niehus and C. Achete, Surf. Sci. **289**, 19 (1993).
[17] D. Farias and K.H. Rieder, Rep. Prog. Phys. **61**, 1575 (1998).
[18] L.J. Gomez, S. Bourgeal, J. Ibanez, and M. Salmeron, Phys. Rev. B **31**, 2551 (1985); R. Kunkel, B. Poelsema, L.K. Verheij, and G. Comsa, Phys. Rev. Lett. **65**, 733 (1991).
[19] J. Camarero *et al.*, Phys. Rev. Lett. **81**, 850 (1998); P. Bonanno, M. Canepa, P. Cantini, R. Moroni, L. Mattera, and S. Terreni, Surf. Sci. **454–456**, 697 (2000).
[20] H. Xu, Y. Yang, and T. Engel, Surf. Sci. **255**, 73 (1991).
[21] P. Dastoor, M. Arnott, E.M. McCash, and W. Allison, Surf. Sci. **272**, 154 (1992).
[22] M. Canepa, S. Terreni, A. Campora, P. Cantini, and L. Mattera, Phys. Rev. B **56**, 4233 (1997).
[23] S. Terreni, P. Cantini, M. Canepa, and L. Mattera, Phys. Rev. B **56**, 6490 (1997).
[24] H.J. Ernst, F. Fabre, and J. Lapujoulade, Phys. Rev. B **46**, 1929 (1992).
[25] C.S. Lent and P.I. Cohen, Surf. Sci. **139**, 121 (1984); P.R. Pukite, C.S. Lent, and P.I. Cohen, *ibid.* **161**, 39 (1985).
[26] M. Henzler, Surf. Rev. Lett. **4**, 489 (1997).
[27] G. Vidali, Surf. Rev. Lett. **4**, 709 (1997).
[28] J.L. Beeby, J. Phys. C **4**, L359 (1977).
[29] C. Mannori, M. Canepa, M.G. Dondi, and F. Tommasini (unpublished).
[30] G. Rosenfeld *et al.*, Surf. Sci. **334**, 1 (1995).
[31] B. Voigtländer, G. Meyer, and N.M. Amer, Phys. Rev. B **44**, 10 354 (1991).
[32] J. de la Figuera, J.E. Prieto, C. Ocal, and R. Miranda, Phys. Rev. B **47**, 13 043 (1993).
[33] M. Xu and R.J. Smith, J. Vac. Sci. Technol. A **9**, 1828 (1991).
[34] B.J. Hinch, C. Koziol, J.P. Toennies, and G. Zhang, Europhys. Lett. **10**, 341 (1989).
[35] S. Löbus, R. Courths, S. Halilov, H. Gollisch, and R. Feder, Surf. Rev. Lett. **3**, 1749 (1996).
[36] P.J. Feibelman and D.R. Hamann, Phys. Rev. B **29**, 6463 (1984).
[37] C. Liu, Y. Park, and S.D. Bader, J. Magn. Magn. Mater. **111**, L225 (1992).
[38] M. Salvietti, R. Moroni, P. Ferro, M. Canepa, and L. Mattera, Phys. Rev. B **54**, 14 758 (1996).